Acta Cryst. (1960). **13**, 35

The Crystal Structure of β-Glycine

BY YŌICHI IITAKA

Department of Mineralogy, The University of Tokyo, Hongo, Tokyo, Japan

(*Received* 6 *April* 1959 *and in revised form* 11 *May* 1959)

The crystal structure of the unstable form of glycine, β, has been determined. The structure was refined by Fourier methods using the (*h*0*l*) and (0*kl*) data obtained by Geiger counter measurements. The crystals are monoclinic with space group $P2_1$ and the unit-cell dimensions are

$$a = 5{\cdot}077,\ b = 6{\cdot}268,\ c = 5{\cdot}380\ \text{Å};\ \beta = 113{\cdot}2°.$$

The structure consists of hydrogen bonded molecular layers, extending parallel to the (010) plane, which have the same configuration of molecules as that found in the α-form. The two forms differ in their hydrogen bond systems between layers.

Introduction

Three polymorphic forms of glycine NH_2CH_2COOH are known. (1) An ordinary form, α, the crystal structure of which was first determined by Albrecht & Corey (1939), a detailed analysis having recently been reported by Marsh (1958). (2) An unstable form, β, first described by Fischer (1905)—Bernal (1931) reported the unit-cell dimensions and space group, but, the space group reported by him is different from the one reported by Ksanda & Tunell (1938). (3) The third form, γ, found by the present author (Iitaka, 1954), the crystal structure of which has recently been determined (Iitaka, 1958, 1959*c*). In this connexion, it seemed worth while to investigate the crystal structure of the β-form so that a comparison might be made among these three crystalline forms, especial interest being paid to their hydrogen bond systems (Iitaka, 1959*a*).

Experimental

β-glycine crystallizes in the form of small needles. These crystals can be obtained by adding ethyl alcohol to a concentrated aqueous solution of glycine. They readily transform into the α-form in air. However, they remain unchanged indefinitely if they are kept in a dry atmosphere.

Rotation and Weissenberg photographs were taken using small crystals, *ca.* 0·1 × 0·3 × 5 mm., which were thoroughly dried and sealed in thin capillary tubes. These photographs exhibit a monoclinic symmetry, with the needle axis as the symmetry axis *b*.

The approximate cell dimensions were obtained from the *b* axis rotation and Weissenberg photographs which were refined using a single crystal diffractometer. They are listed in Table 1. The only systematic absences observed are (0*k*0) reflections with *k* odd, thus confirming the results of Ksanda & Tunell (1938). The crystals were tested for piezoelectricity by the vibrating electrode method (Iitaka, 1953), and were found to have definite piezoelectric property. The only possible space group is $P2_1$. In Table 1, the cell dimensions, space groups, and molecular volumes are given together with the values previously obtained for α and γ glycine.

Intensity data were recorded for both (0*kl*) and (*h*0*l*) planes with Cu $K\alpha$ radiation using a single crystal diffractometer (Iitaka, 1959*b*). The integrated intensities were corrected for Lorentz and polarization factors, but the correction for absorption was considered unnecessary.

Determination of the trial structure

As shown in Table 1, the lengths of the *a*- and *c*-axis of the β-form are very close to those of the α-form while the *b*-axis is almost halved. Since the crystals of α-glycine are made up of layers of molecules extending parallel to the (010) plane, which are stacked in four layers along the *b*-axis, it was suggested that the crystal structure of β-glycine is formed by two such layers stacking along the *b*-axis.

In attempting to find the location of the molecules,

Table 1. *Comparison of the cell dimensions and space groups of α-, β- and γ-glycine*

Form	Cell size in Å				Volume (Å³)	Space group	*Z*	Molecular volume (Å³)
	a	*b*	*c*	β				
α*	$5{\cdot}102_0$	$11{\cdot}970_9$	$5{\cdot}457_5$	111° $42'_3$	$309{\cdot}6_9$	$P2_1/n$	4	$77{\cdot}4_2$
β	$5{\cdot}077_4$	$6{\cdot}267_6$	$5{\cdot}379_9$	113° 12′	$157{\cdot}3_6$	$P2_1$	2	$78{\cdot}6_8$
γ†	7·037		5·483		$235{\cdot}1_4$	$P3_1$ or $P3_2$	3	$78{\cdot}3_8$

* Marsh (1958). † Iitaka (1958).

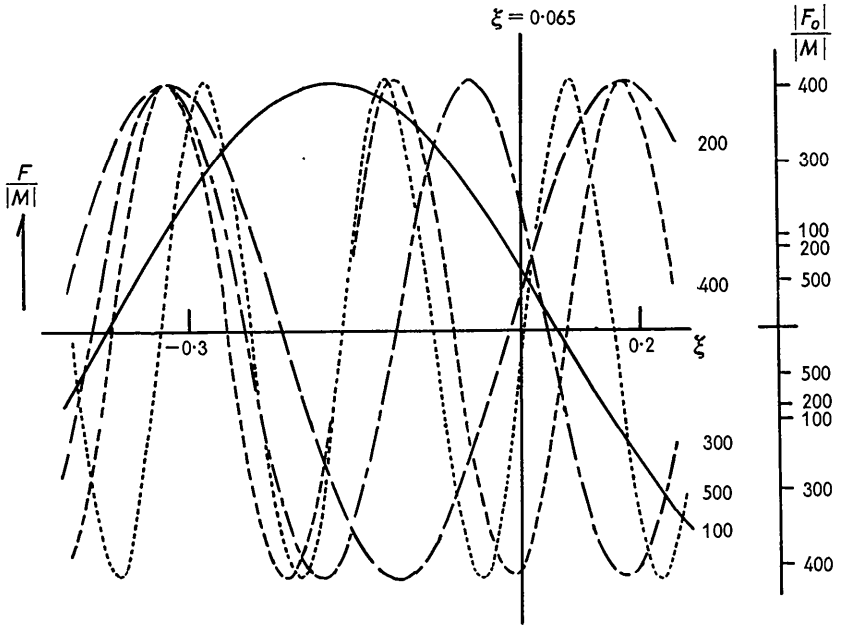

Fig. 1. Variation of the (h00) structure amplitudes by the translation of the molecules. The numbers 100 etc. indicate the indices of (h00) planes.

it was assumed that the dispositions of the atoms in the molecule were the same as those found in the α-form, and its Fourier transforms for several zones were calculated. Since the space group is $P2_1$ the structure factors for the ($h0l$) planes can be expressed by

$$F(h0l)=2\sum_{n=1}^{N} f_n \cos 2\pi\{h(\xi+x_n)+l(\zeta+z_n)\}$$
$$=|M(h0l)|\cos\{2\pi(h\xi+l\zeta)+\varphi\},$$
$$|M(h0l)|=2\left[\left\{\sum_n^N f_n \cos 2\pi(hx_n+lz_n)\right\}^2+\left\{\sum_n^N f_n \sin 2\pi(hx_n+lz_n)\right\}^2\right]^{\frac{1}{2}}$$
$$\tan\varphi=\sum_n^N f_n \sin 2\pi(hx_n+lz_n)\Big/\sum_n^N f_n \cos 2\pi(hx_n+lz_n),$$

where x_n, z_n are the coordinates of the atoms with reference to a chosen origin fixed to the molecule and ξ, ζ are the components of the translation vector of the molecule with respect to the symmetry center. If the orientation of the molecule is assumed to be the same as in the α-form, the variation of the structure amplitudes by the translation of the molecule will be represented by a simple diagram. An example is shown in Fig. 1, which shows how $F/|M|$ varies with ξ for different values of h. The location of the molecule was found by fitting the relative values of $|F_o|/|M|$ to the curves. Approximate y coordinates were obtained by adopting similar molecular dispositions as in the α-form.

Structure factors were calculated for this trial structure, and the reliability factors 30·6% for ($h0l$) and 36·2% for ($0kl$) reflexions were obtained. The scaling and temperature factors for both zones were found by plotting the values $\ln(F_c/F_o)$ against $1/d^2$. The slope of the graphs gave an overall temperature factor $B=3{\cdot}5$ Å^2. The electron-density projection $\varrho(x, z)$ was computed from the observed coefficients with signs determined by the trial structure. The resolution of the atoms was not quite good owing to overlapping. It is shown in Fig. 2.

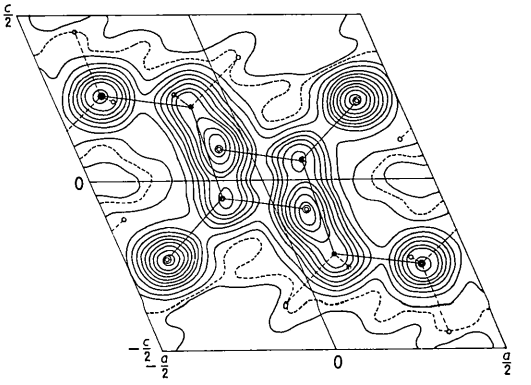

Fig. 2. The b-axis Fourier projection for β-glycine.

Refinement of the structure

The refinement of the structure was carried out by the successive use of difference Fourier projections (Cochran, 1951) along the b- and a-axis. Throughout the work the atomic scattering factors given by Berghuis *et al.* (1955) were used.

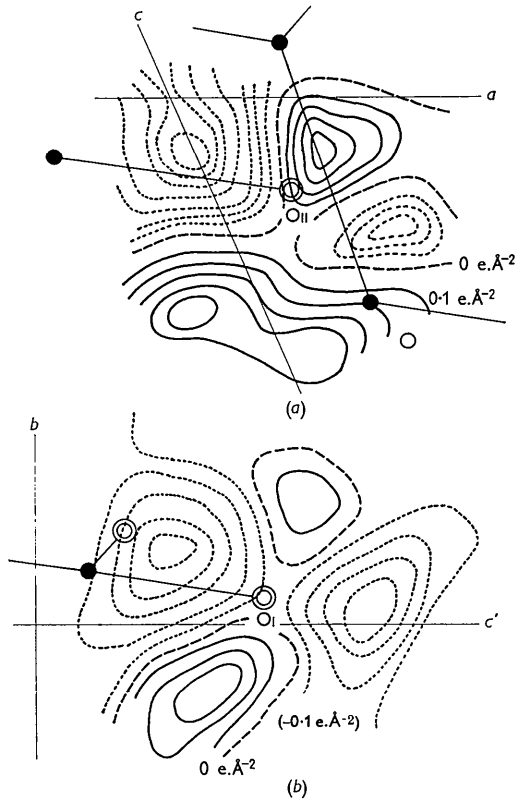

Fig. 3. A portion of the difference maps showing the anisotropic thermal motions of the oxygen atoms. (*a*) The *b*-axis, (*b*) the *a*-axis projection.

By the fourth cycle in the (*h*0*l*) projection, most of the signs of the structure amplitude were determined and the x and z atomic coordinates were improved sufficiently to reduce the R factor to 18·5%. A subsequent difference synthesis showed a considerable overlap of hydrogen atoms attached to the nitrogen and methylenic carbon atoms so that the location of these hydrogen atoms proved to be difficult. The hydrogen atoms were then included at the assumed positions which gave a C–H length of 1·10 Å and a N–H length of 1·00 Å with a tetrahedral arrangement with respect to the N–C bond. The resulting R factor was reduced to 14·5%. After two cycles of refinement using difference synthesis in which calculated structure factors included the contributions from the five hydrogen atoms, the R factor dropped to 13·9%.

At this stage, it became clear that further changes in the coordinates would effect little improvement, and the difference maps gave a clear indication of anisotropic thermal motions of the oxygen atoms (Fig. 3(*a*)). The temperature factor here takes the form as shown in Table 4. The constants B_1 and B_2 were determined assuming the parabolic forms of the difference maps near the center of atoms. Three cycles of refinement were then carried out including the anisotropic temperature factor parameters for the two oxygen atoms (O_I and O_{II}). The R factor was reduced to 10·4%.*

For the *a*-axis projection, on the other hand, by the seventh cycle the R factor dropped to 12·3%, which was further reduced to 11·2% when the hydrogen atoms were included. In a difference Fourier plot, marked anisotropic thermal vibration of the oxygen atom O_I was indicated, the direction of the maximum thermal vibration being inclined about 17° from the *b*-axis (Fig. 3(*b*)). Further four cycles of refinement were carried out including the anisotropic temperature factor parameters for the oxygen O_I, nitrogen

* 9·1%, excluding (001), (101) and (002) planes which were affected by extinction.

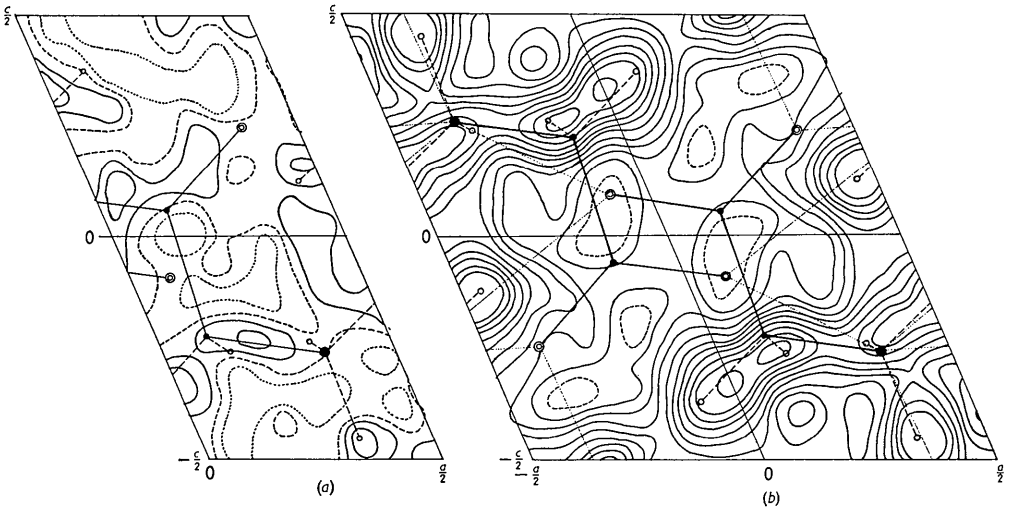

Fig. 4. The final difference Fourier maps for the *b*-axis projection. Contours at intervals of 0·1 e.Å^{-2}. Broken lines indicate 0 e.Å^{-2}. Dotted lines indicate negative contours. (*a*) The contribution of the hydrogen atoms to the values F_c included. (*b*) The contribution of the hydrogen atoms to the values F_c omitted.

and the methylenic carbon C_{II} atoms; with the latter two atoms the direction of the maximum thermal vibration was assumed to be parallel to the *b*-axis. The resulting *R* factor was 8·2%.*

At this stage, it was noted that the strong intensities all had consistently higher calculated values. It was presumed that this discrepancy was caused by extinction and the following corrections were applied (Darwin, 1922).

$$I_{cor.} = I_0/(1-gI_0)\,,$$

where I_0 denotes the observed intensity and g is a constant. g was found by plotting $Lp|F_c|^2/I_0$, against $Lp|F_c|^2$, for many reflexions and the values $g = 6{\cdot}6\times10^{-4}$ and $4{\cdot}0\times10^{-4}$ were obtained for (*h*0*l*) and (0*kl*) reflexions, respectively. Comparison of the corrected observed structure factors with the calculated ones gave the *R* factors 7·8% and 4·3% for (*h*0*l*) and (0*kl*) planes, respectively.

The scale factors and overall temperature factors for both projections were now recalculated by the method described earlier. A subsequent difference map† for the *b*-axis projection indicated some anisotropic thermal motions of the atoms N and C_I, whereas no significant change was found on the *a*-axis projection.

For the (*h*0*l*) reflexions, individual anisotropic temperature factor parameters were now introduced for the atoms N, C_I, O_I and O_{II}, and five cycles of refinement were carried out. The *R* factors decreased steadily to 4·6% (9·9% if hydrogen atoms are not included). The final difference Fourier maps* are shown in Fig. 4.

For the (0*kl*) reflexions, after slight adjustment of the isotropic temperature factor for the oxygen atom O_{II}, the final difference map* was computed, in which the contribution of the hydrogen atoms to the values of F_c had been omitted. All the positions where hydrogen atoms are expected had their peaks 0·4 ~ 0·5 e.Å^{-2} in height, but they were not clearly resolved, owing to the non-centrosymmetric nature of this projection.

A comparison of the final calculated and observed structure factors is given in Table 2. The final atomic parameters† and temperature factors for the atoms in one asymmetric unit are listed in Table 3 and Table 4.

The standard deviations of the electron density were estimated by the equation (Lipson & Cochran, 1953; Cruickshank, 1949)

* 5·6%, excluding (020) plane.

† Including all terms but giving the weight ½ for those planes which were corrected for extinction.

* Including all terms but giving the weight ½ for those planes which were corrected for extinction.

† Hydrogen atoms are placed at the geometrically assumed positions.

Table 2. *Observed and calculated structure factors*

*h*0*l*	$\|F_o\|$	F_c with *H*	F_c without *H*	*h*0*l*	$\|F_o\|$	F_c with *H*	F_c without *H*
100	7·59*	7·20	8·28	$\bar{4}03$	0·0	−0·25	−0·32
200	2·98	2·47	1·66	$\bar{3}03$	2·70	−2·75	−3·21
300	3·08	2·76	2·56	$\bar{2}03$	2·28	1·80	1·41
400	12·80*	−13·09	−12·72	$\bar{1}03$	1·85	1·36	−0·37
500	1·86	−2·04	−2·06	003	2·16	−1·88	−1·53
				103	1·92	−2·07	−2·26
$\bar{6}01$	0·0	0·55	0·56	203	3·32	−3·40	−3·23
$\bar{5}01$	2·20	−2·41	−2·70	303	0·97	0·87	1·02
$\bar{4}01$	9·08	−9·16	−9·63				
$\bar{3}01$	8·36	−8·28	−7·83	$\bar{6}04$	0·0	0·19	0·10
$\bar{2}01$	8·32*	−8·41	−8·89	$\bar{5}04$	0·80	1·13	1·16
$\bar{1}01$	5·94	5·94	8·73	$\bar{4}04$	7·47	−7·41	−7·24
001	20·80*	20·33	21·78	$\bar{3}04$	4·34	4·18	4·02
101	18·01*	18·88	18·45	$\bar{2}04$	1·04	1·03	1·72
201	10·20*	10·16	10·28	$\bar{1}04$	5·93	−6·00	−6·14
301	1·70	−1·44	−1·18	004	6·71	6·34	6·30
401	0·0	−0·01	−0·12	104	4·49	−4·41	−4·50
501	2·13	−1·98	−1·89	204	3·27	−3·14	−3·14
				304	1·82	2·00	1·96
$\bar{6}02$	0·0	−0·41	−0·37				
$\bar{5}02$	3·95	−4·08	−4·08	$\bar{5}05$	1·28	1·23	1·19
$\bar{4}02$	2·88	2·87	3·02	$\bar{4}05$	0·77	−0·82	−0·80
$\bar{3}02$	14·41*	−14·49	−14·87	$\bar{3}05$	0·70	0·62	0·84
$\bar{2}02$	6·93	−7·01	−5·84	$\bar{2}05$	1·18	−0·99	−1·11
$\bar{1}02$	11·87*	11·94	12·09	$\bar{1}05$	1·56	−1·30	−1·08
002	17·2*	−17·31	−16·29	005	1·90	−1·70	−1·67
102	9·91*	10·52	10·92	105	1·12	−1·22	−1·37
202	5·33	5·29	4·75				
302	3·02	−3·12	−3·20	$\bar{4}06$	6·26	5·96	5·88
402	5·01	5·26	5·06	$\bar{3}06$	0·0	0·08	0·07
				$\bar{2}06$	0·0	−0·66	−0·76
$\bar{6}03$	1·20	−1·00	−0·89	$\bar{1}06$	1·10	1·32	1·27
$\bar{5}03$	2·34	−2·57	−2·47	006	5·65	−5·46	−5·40

Table 2 (*cont.*)

			F_c with H			F_c without H	
$0kl$	$\|F_o\|$	$\|F_c\|$	$\cos\alpha$	$\sin\alpha$	$\|F_c\|$	$\cos\alpha$	$\sin\alpha$
001	20·8*	20·33	1·000	0·000	21·78	1·000	0·000
002	17·2*	17·31	−1·000	0·000	16·29	−1·000	0·000
003	2·16	1·88	−1·000	0·000	1·53	−1·000	0·000
004	6·71	6·34	1·000	0·000	6·30	1·000	0·000
005	1·90	1·70	−1·000	0·000	1·67	−1·000	0·000
006	5·65	5·46	−1·000	0·000	5·40	−1·000	0·000
011	6·17	5·40	−0·968	0·253	6·77	−0·788	0·616
012	12·62*	13·30	−0·339	0·941	12·81	−0·329	0·944
013	9·07	9·45	−0·322	0·947	10·02	−0·299	0·954
014	4·43	4·65	−0·574	0·819	4·62	−0·602	0·799
015	1·53	1·60	−0·621	0·784	1·59	−0·621	0·784
016	0·70	0·90	0·669	0·743	0·90	0·690	0·724
020	42·3*	41·7	0·894	0·448	40·95	0·883	0·469
021	15·18*	15·16	0·629	0·777	15·68	0·663	0·749
022	9·96	9·85	−0·989	0·146	11·16	−0·993	0·120
023	1·62	1·70	−0·473	−0·881	1·74	−0·378	−0·926
024	4·90	4·78	0·990	−0·139	4·94	0·994	−0·111
025	1·16	0·89	−0·775	−0·633	0·88	−0·778	−0·628
031	9·91	9·41	−0·970	0·242	9·40	−0·949	0·314
032	6·34	6·55	−0·876	0·482	6·55	−0·891	0·454
033	3·42	3·71	−0·990	0·143	3·86	−0·965	0·262
034	4·51	4·79	−0·998	0·062	4·76	−0·999	0·052
035	2·62	2·89	−0·912	0·410	2·86	−0·916	0·400
040	11·62*	12·01	0·310	0·951	11·72	0·309	0·951
041	8·04	7·70	−0·116	0·993	7·52	−0·088	0·996
042	4·40	3·88	−0·963	0·270	3·82	−0·943	0·332
043	1·38	1·04	0·232	−0·973	1·08	0·262	−0·965
044	2·34	2·41	0·993	−0·120	2·45	0·993	−0·121
045	0·0	0·73	0·662	−0·749	0·75	0·659	−0·752
051	4·57	4·86	−0·988	0·154	5·09	−0·975	0·220
052	2·74	2·79	−0·894	−0·448	2·78	−0·889	−0·459
053	3·23	3·47	−0·278	−0·961	3·41	−0·266	−0·964
054	3·18	3·19	−0·852	−0·524	3·24	−0·850	−0·527
060	4·30	4·35	−0·788	0·615	4·49	−0·792	0·610
061	3·28	3·28	−0·752	0·659	3·25	−0·751	0·660
062	0·67	0·96	−0·553	0·833	1·00	−0·596	0·803
063	0·43	0·19	0·977	−0·213	0·22	0·935	−0·355
071	1·78	2·05	−0·969	0·247	2·02	−0·967	0·257
072	1·20	1·10	−0·216	−0·977	1·10	−0·216	−0·977

* Corrected for extinction.

$$\sigma(\varrho)=(\pi S_0^2/A)^{\frac{1}{2}}\sigma(F_o)\,,\quad \sigma(F_o)=\Big[\sum_q (F_o-F_c)^2/q\Big]^{\frac{1}{2}}\,,$$

where q is the number of all independent terms which lie within a sphere of S_0 in the reciprocal lattice.

Table 3. *Final positional parameters*

	x	y	z
N	0·3522	−0·0440	−0·2619
O_I	0·3772	0·0270	0·2420
O_{II}	−0·0896	0·0773	0·0970
C_I	0·1378	0·0532	0·0633
C_{II}	0·1145	0·0719	−0·2265
H_I (NH_3^+)	0·540	0·012	−0·135
H_{II} (NH_3^+)	0·340	−0·031	−0·449
H_{III}(NH_3^+)	0·337	−0·203	−0·216
H_I (CH_2)	0·125	0·241	−0·274
H_{II} (CH_2)	−0·091	0·008	−0·362

Table 4. *Final anisotropic temperature factor parameters*

The temperature factors take the following form

$$\exp -B\,(\sin\theta/\lambda)^2,\quad B=B_1+B_2\sin^2(\omega-\varphi)$$

	B (Å²) for ($h0l$) projection	B (Å²) for ($0kl$) projection
N	$1·96+0·40\sin^2(\omega+70°)$	$2·32+1·73\sin^2\omega$
O_I	$2·23+0·30\sin^2(\omega-12°)$	$1·97+3·15\sin^2(\omega+17°)$
O_{II}	$1·69+1·89\sin^2(\omega+70°)$	3·36
C_I	$2·63+0·10\sin^2\omega$	2·63
C_{II}	2·83	$2·83+0·96\sin^2\omega$

where (s,ω), $s=2\sin\theta/\lambda$, are the polar coordinates of a point in the reciprocal lattice referred to the c^* axis.

For the hydrogen atoms different temperature factor parameters were used for each projection

$$B(h0l)=2·00\text{ Å}^2,\quad B(0kl)=3.44\text{ Å}^2.$$

Using the values $S_0=1{\cdot}270$ Å^{-1}, $A(h0l)=25{\cdot}10$ Å^2, $A(0kl)=31{\cdot}00$ Å^2, $\sigma F_o(h0l)=0{\cdot}277$, $\sigma F_o(0kl)=0{\cdot}317$, the standard deviations were found to be $\sigma(\varrho)=0{\cdot}124$ e.Å^{-2} for the $(h0l)$ projection and $\sigma(\varrho)=0{\cdot}127\times 2=0{\cdot}254$ e.Å^{-2} for the $(0kl)$ projection. The latter was multiplied by two, since the projection has no center of symmetry.

The standard deviations of the atomic coordinates were estimated by the equation.

$$\sigma(x_n)=\left(\frac{\pi S_0^2}{A}\cdot\frac{\pi^4}{4p_n^4}\right)^{\frac{1}{2}}\frac{S_0}{Z_n}\,\sigma(F_o)\,.$$

Although small variation was found from atom to atom, the average standard deviations of the atomic coordinates were obtained by taking $p_n=4{\cdot}0$ Å^{-2} and $Z_n=6$, to be $\sigma(x_n)$, $\sigma(z_n)=0{\cdot}008$ Å and $\sigma(y_n)=0{\cdot}017$ Å.

As the anisotropic thermal vibrations of the two oxygen atoms are appreciable, slight corrections are necessary to allow for the angular oscillations which cause the atoms to appear too close to the center of the oscillation (Cruickshank, 1956). The shortening of the C–O bond lengths was estimated by (1) taking the maximum B value for each oxygen atom in a direction perpendicular to the C–O bond, (2) subtracting the mean B value for the C_I atom (since the anisotropic thermal vibration of the C_I atom is small), and (3) calculating the mean-square amplitude of vibration by the formula $\overline{u^2}=B/8\pi^2$ whereupon, the mean-square amplitudes obtained were 0·012 Å^2 (in the xz plane) for the atom O_I, and 0·032 Å^2 (in the yz' plane) for O_{II}. In this manner the following shortening was estimated: for the C_I–O_I bond taking $s^2=0{\cdot}012$ Å^2, $t^2=0$ Å^2, $p=4{\cdot}5$ Å^{-2} and $r=1{\cdot}228$ Å giving $\Delta r=0{\cdot}0045$ Å, while for the C_I–O_{II} bond taking $s^2=0$ Å^2, $t^2=0{\cdot}032$ Å^2, $p=4{\cdot}5$ Å^{-2} and $r=1{\cdot}247$ Å, Δr found to be 0·0099 Å. In Table 5, the corrected bond lengths are indicated by asterisks.

Description and discussion of the structure

Molecular configuration

The bond distances and angles in β-glycine, calculated from the parameters listed in Table 3, are given in Table 5 together with the values for α-glycine.

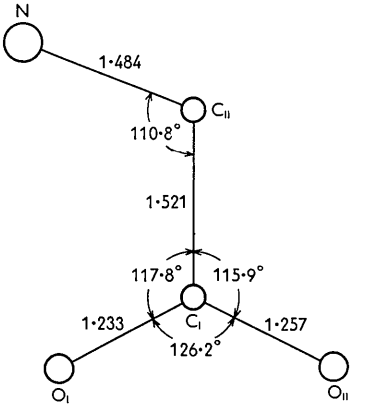

Fig. 5. Bond lengths and angles of glycine molecules found in the β-form.

Table 5. *Bond lengths and angles in glycine molecules*

	β-form	α-form†		β-form	α-form†
N–C_{II}	1·484 Å	1·474 Å	C_I–C_{II}–N	110·8°	111·8°
C_{II}–C_I	1·521	1·524	O_I–C_I–O_{II}	126·2	125·5
C_I–O_I	1·233*	1·252 (1·261*)	C_{II}–C_I–O_I	117·8	117·4
C_I–O_{II}	1·257*	1·255 (1·265*)	C_{II}–C_I–O_{II}	115·9	117·1

* Corrected for rotational oscillations of the molecule. † Marsh (1958).

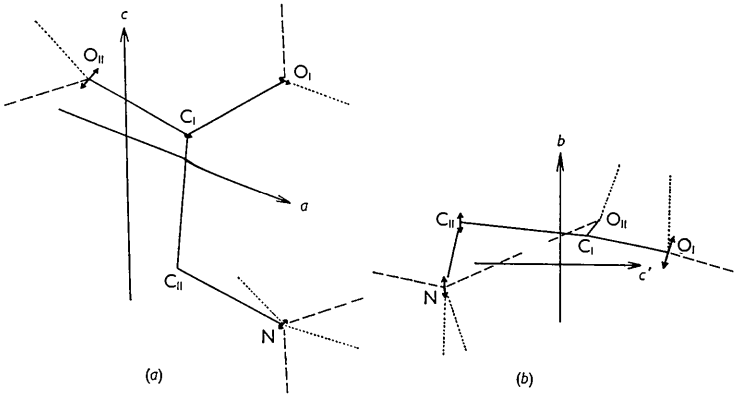

Fig. 6. Schematic illustrations of the anisotropic thermal motions of the molecule. Arrows indicate the direction and the magnitude of the root mean-square amplitude of the anisotropic thermal vibration. (*a*) The *b*-axis projection. (*b*) The *a*-axis projection. Broken lines indicate hydrogen bonds. Dotted lines indicate a bifurcated hydrogen bond.

The standard deviations in bond lengths and angles, calculated from the standard deviations of the positional parameters, are about 0·015 Å and 0·9°. The values for the bond distances and angles are close to those found in the α-form. However, the departure of the nitrogen atom from the plane containing the carboxyl group by 0·583 Å* is somewhat larger than the value 0·436 Å,* reported for the α-form. This difference is presumably explained by the fact that the direction of the interlayer hydrogen bond attached to the O_I atom is in a sense opposite to that in the α-form. The N–O_I distance is 2·701 Å whereas it is 2·690 Å in the α-form. The C–N bond found in this investigation, 1·484 Å, is of a typical value of αC–N distance found in amino acids and their related compounds (L-threonine, 1·49 Å (Shoemaker, Donohue, Schomaker & Corey, 1950): DL-alanine, 1·50 Å (Donohue, 1950): N,N′-diglycyl-cystine, 1·46 Å (Yakel & Hughes, 1952): DL-serine, 1·49 Å (Shoemaker, Barieau *et al.*, 1953): glycyl-*l*-asparagine, 1·46 Å (Pasternak, Katz & Corey, 1954)).

The bond distances and bond angles suggest that the molecule exists as a zwitter ion. This view was further supported by the difference Fourier map (Fig. 4), which will be discussed later.

The atoms within the carboxyl group and the methylenic carbon atom are almost coplanar; the deviation for the carboxyl carbon atom from the best plane containing the two oxygen and the two carbon atoms is 0·018 Å. The C_I–O_I bond, 1·233 Å, found in this investigation is slightly shorter than the values found in the α-form (1·261 Å). The difference is, however, almost within the limit of experimental error.

It is evident that in the β-form one and the same kind of asymmetric molecules crystallize into one of the enantiomorphous forms as in the γ-form, whereas in the α-form two enantiomorphous molecules are related by a center of symmetry as in the case of racemic acid.

Anisotropic thermal motions of the molecule

The anisotropic thermal vibrations of the atoms may be interpreted to be due, in part, to the anisotropic thermal motions of the molecule as a whole. A comprehensive illustration of the anisotropic thermal motions is given in Fig. 6, which shows the values of the root mean square amplitude of the anisotropic part (B_2 in Table 4) in the direction parallel to the maximum vibration. If we assume that the anisotropic movement consists of an oscillation of the molecule in its own plane and a libration out of the plane about the mass center of the molecule, the anisotropic thermal vibrations of the atoms can be satisfactorily explained.

* The departure of the nitrogen atom from the least-squares plane containing the atoms C_I, C_{II}, O_I and O_{II}.

Framework features

In Fig. 7, a view of the structure parallel to the *c*-axis is shown together with that of the α-form.

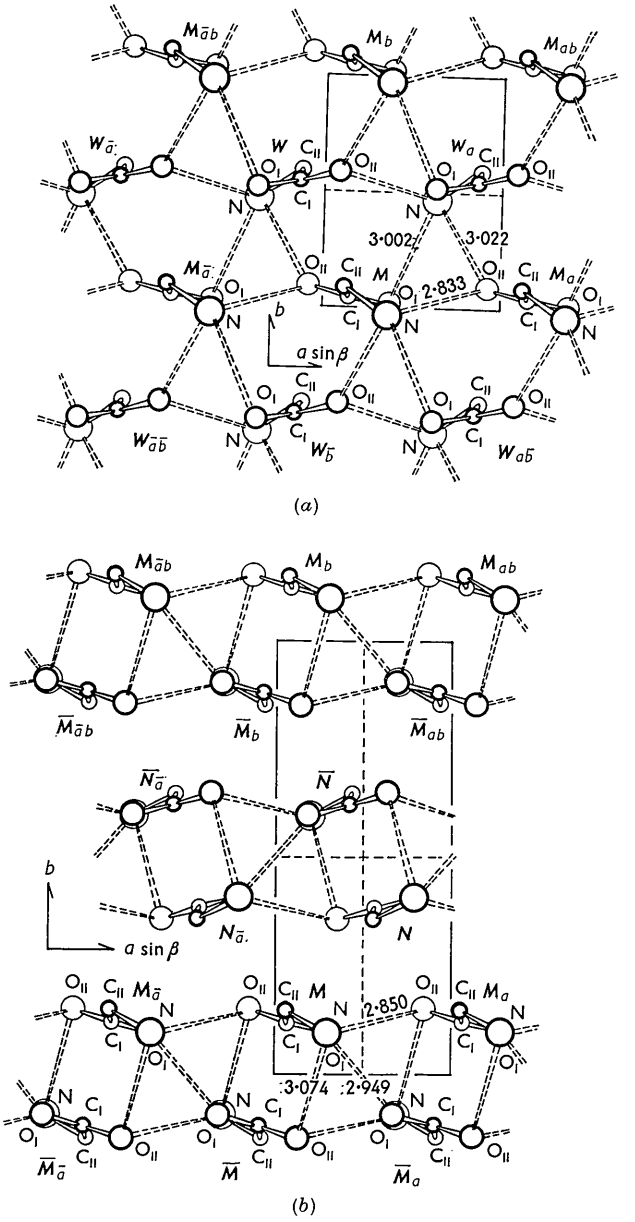

Fig. 7. Views of crystal structure of glycine parallel to the *c*-axis. (*a*) β-glycine. (*b*) α-glycine (after Albrecht & Corey, 1939).

It may be seen that the structures of both forms consist of molecular layers extending parallel to the (010) planes. Fig. 8 is the projection of β-glycine onto the (010) plane, which shows a network of N–H · · · O hydrogen bonds in the (010) plane holds the nearly flat molecules together to form the extended sheets. The configuration of the sheet in α-glycine is almost the same. In β-glycine, these single sheets are packed

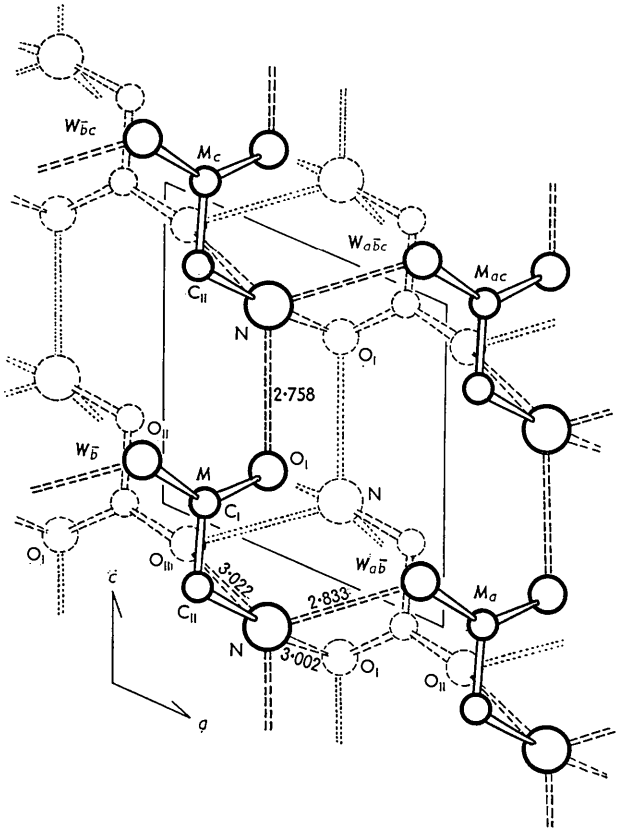

Fig. 8. A projection upon the (010) plane showing a network of hydrogen bonds in a molecular layer of β-glycine.

together by hydrogen bonds extensively in the *b*-direction; whereas in α-glycine, two single sheets are held together by hydrogen bonds to form a double sheet, which is packed by van der Waals forces throughout the crystal.

Hydrogen bonds

Around a nitrogen atom, there are four oppositely charged oxygen atoms of immediate neighbours at short distances. They are listed in Table 6. Among these, two oxygen atoms in the same layer ($O_I^{M\bar{c}}$ and O_{II}^{Ma}) are arranged approximately in tetrahedral directions with respect to the N–C bond, and they are so close to the nitrogen atom (see Table 6) that they undoubtedly take part in hydrogen bonds. In fact, the difference map shows two peaks on the lines connecting the nitrogen and two oxygen atoms, $N\cdots O_I^{M\bar{c}}$ and $N\cdots O_{II}^{Ma}$, at distances about 1 Å from the nitrogen atom. The same map also shows another peak at about 1 Å from the nitrogen atom, on the line bisecting the angle $O_I^{Wa\bar{b}}$–N–$O_{II}^{W\bar{b}}$. These three hydrogen peaks are situated almost tetrahedrally with respect to the N–C bond. It is suggested that the third hydrogen atom plays the role of a bifurcated hydrogen bond, similar to the interlayer hydrogen bond found in the α-form.

Table 6. N · · · O *interatomic distances, and* C–N · · · O *angles*

β-form

	$N\cdots O_I^{M\bar{c}}$	$N\cdots O_{II}^{Ma}$	$N\cdots O_I^{Wa\bar{b}}$	$N\cdots O_{II}^{W\bar{b}}$
N···O (Å)	2·758	2·833	3·002	3·022
C–N···O (°)	113·3	115·4	144·9	82·6

α-form*

	$N\cdots O_I^{M\bar{c}}$	$N\cdots O_{II}^{Ma}$	$N\cdots O_I^{\bar{M}a}$	$N\cdots O_{II}^{\bar{M}}$
N···O (Å)	2·768	2·850	2·949	3·074
C–N···O (°)	118·0	116·1	155·8	93·0

* Marsh (1958).

It will be noted that the infrared spectra of these crystals obtained with fine powder specimens (prepared by rapid precipitation) indicate some significant frequency differences for the highest N–H stretching vibration. The spectra observed in the region 2800 cm.$^{-1}$ ~ 3300 cm.$^{-1}$ are shown in Fig. 9. The absorption occurring at 3154 cm.$^{-1}$ in α-glycine corresponds to the highest N–H stretching frequency. This absorption shifts to a lower value, 3093 cm.$^{-1}$, in γ-glycine, and shifts to a higher value, 3180 cm.$^{-1}$, in β-glycine. It has been suggested* that the shift in γ-glycine may be interpreted as indicating that the weakest hydrogen bond in the α-form is weaker than the weakest hydro-

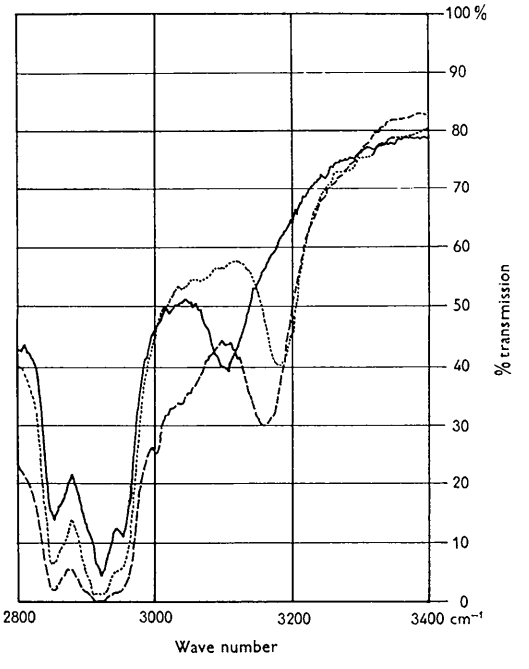

Fig. 9. Infrared spectra observed in a region 2800 cm.$^{-1}$~3300 cm.$^{-1}$. Dotted line: β-glycine. Broken line: α-glycine. Full line: γ-glycine (three peaks in a region 2800 cm.$^{-1}$~3000 cm.$^{-1}$ are due to absorption by nujol).

* Private communications from Dr Tsuboi. For infra-red spectra of these crystals, see Tsuboi *et al.* (1958).

Table 7. *Interatomic distances between molecules of glycine*

β-form

	Same layer		Between layers			
			M and W		M and $W_{\bar{b}}$	
	From M to	Distance	From M to	Distance	From M to	Distance
NH_3–O_I	$M_{\bar{c}}$	2·758 Å	W_a	3·820 Å	$W_{a\bar{b}}$	3·002 Å
NH_3–O_{II}	M_a	2·833	W	4·320	$W_{\bar{b}}$	3·022
	$M_{\bar{c}}$	3·378				
NH_3–CH_2	M_a	3·868	W_a	4·851	$W_{a\bar{b}}$	3·798
			$W_{\bar{c}}$	4·791	$W_{\bar{b}\bar{c}}$	3·721
NH_3–NH_3			W_a	4·084	$W_{a\bar{b}}$	4·084
			$W_{a\bar{c}}$	4·655	$W_{a\bar{b}\bar{c}}$	4·655
			$W_{\bar{c}}$	4·686	$W_{\bar{b}\bar{c}}$	4·686
CH_2–CH_2			W	4·398	$W_{\bar{b}}$	4·398
			$W_{\bar{c}}$	4·140	$W_{\bar{b}\bar{c}}$	4·140
O_I–CH_2	M_c	3·611	W	4·212	$W_{\bar{b}}$	3·770
	M_{ac}	3·720	W_a	4·301	$W_{a\bar{b}}$	3·870
O_{II}–CH_2	M_c	3·369	W	3·191	$W_{\bar{b}}$	3·257
O_I–O_{II}	M_a	3·115	W	3·906	$W_{\bar{b}}$	3·362
O_I–O_I			W_{ac}	4·044	$W_{a\bar{b}c}$	4·044
			W_a	4·551	$W_{a\bar{b}}$	4·551
O_{II}–O_{II}			W	3·534	$W_{\bar{b}}$	3·534

α-form*

	Same layer		Between layers			
			M and $\bar{M}$		M and N	
	From M to	Distance	From M to	Distance	From M to	Distance
NH_3–O_I	$M_{\bar{c}}$	2·768 Å	$\bar{M}_a$	2·949 Å		
NH_3–O_{II}	M_a	2·850	$\bar{M}$	3·074	$N_{\bar{c}}$	3·330 Å
	$M_{\bar{c}}$	3·427				
NH_3–CH_2	M_a	3·869	$\bar{M}_a$	4·338	N	4·220
			$\bar{M}_{\bar{c}}$	3·965	$N_{\bar{c}}$	4·528
NH_3–NH_3			$\bar{M}_a$	3·533	$N_{\bar{a}\bar{c}}$	4·849
			$\bar{M}_{\bar{c}}$	3·875		
			$\bar{M}_{a\bar{c}}$	4·428		
CH_2–CH_2			$\bar{M}$	4·363	N	3·890
			$\bar{M}_{\bar{c}}$	4·557		
O_I–CH_2	M_c	3·697	$\bar{M}$	3·410	N	3·362
	M_{ac}	3·977	$\bar{M}_a$	4·336		
O_{II}–CH_2	M_c	3·460	$\bar{M}$	3·477	$N_{\bar{a}}$	3·272
O_I–O_{II}	M_a	3·167	$\bar{M}$	3·316	N	3·717
O_I–O_I			$\bar{M}_{ac}$	3·622	N	4·766
			$\bar{M}$	3·937		
O_{II}–O_{II}			$\bar{M}$	4·053	N	3·943

* Calculated from the data published by Marsh (1958).

gen bond in the γ-form. It may be equally said that the weakest hydrogen bond in the β-form is weaker than the corresponding hydrogen bond in the α-form. Since these absorption bands may be assigned to the N–H stretching vibrations associated with the inter-layer or inter-chain hydrogen bonds, the inference is that in β-glycine each single layer is held to one another by weaker hydrogen bonds than those contributing to the formation of the double layer in the α-form.

Packing of the molecules

In Table 1, the molecular volumes are listed, which were calculated from the lattice constants and the number of molecules contained in the unit cell. It is noted that the β-form has the largest volume, which means that the packing of the molecules in the β-form is somewhat loose. Of especial interest in this connexion is the directional property of the hydrogen bonds and the extent to which this particular property is respon-

sible for the packing of the molecules in the two forms. In Fig. 7, three types of molecules related to M by a two-fold screw axis, a center of symmetry and an n glide plane are designated respectively W, $\bar{M}$ and N, and all other molecules which are related to these four by lattice translations are designated with subscript denoting the translation vector. The interatomic distances between molecules of glycine are summarized in Table 7. Fig. 10 shows the packing of molecules, for β, in the layer containing M with some other molecules in the adjacent layer. In this figure, CH_2, NH_3 and O are drawn with the van der Waals radii of 2·0, 1·8 and 1·35 Å respectively.

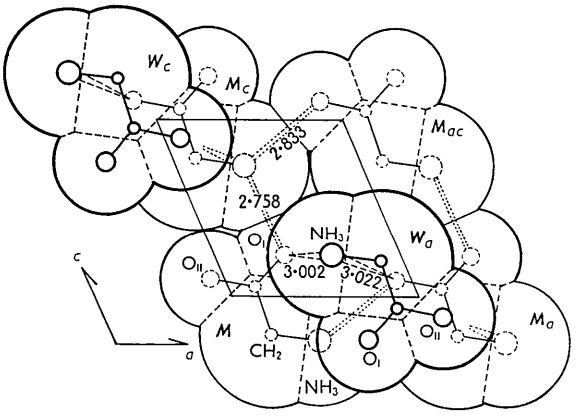

Fig. 10. Packing drawing of the molecular layers viewed along the b-axis. Only two layers, M and W are shown.

In β-glycine, the packing of molecules within the layer is rather compact as can be seen from Table 7. Between the layers M and W, the directional property of the hydrogen bonds is not fully satisfied and rather weak bifurcated hydrogen bonds are formed. The feature which prevents the formation of shorter hydrogen bond between layers may be the methylene–oxygen or methylene–methylene contacts between layers. In facts, as shown in Fig. 7(a) and Fig. 10, two molecules related by a screw axis are displaced in such a way that bulky methylene groups fit nearly into gaps in the adjacent layer. In the case of α-glycine, the nitrogen atoms are buried within the double layer, and the close contacts between the double layers take place between oxygen atoms and methylene groups or between methylene groups.

To conclude the discussion, it must be pointed out that the β-form readily transforms, irreversibly, into the α- or the γ-forms. The change that take place during the transformation, β to α, is surprising. A comparison of the structure of the two forms can most easily be made by inspecting Fig. 7(a) and (b). We shall designate the layers in which the nitrogen atoms are pointing to the $+c$ direction by a sign (+), and the reverse by (−). In β-glycine, the stacking sequence of the layer can be represented by (+)(−)(+)(−)..., whereas it is (+)(−)(−)(+)(+)(−)... in α-glycine.

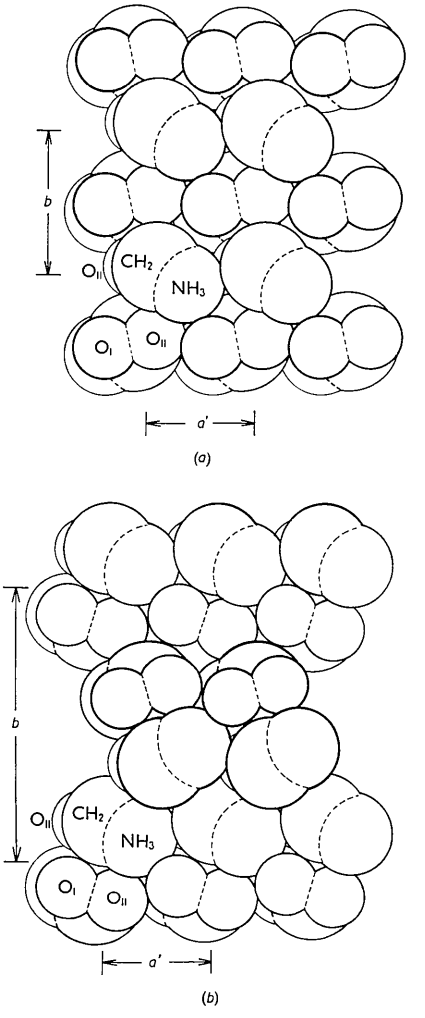

Fig. 11. Packing drawings of the molecular layers viewed along the c-axis. (a) β-glycine. (b) α-glycine (after Albrecht & Corey, 1939).

In order to convert the β-form into α, the molecules in every other layer should flop over from one enantiomorphic form to the other. This may effect the formation of the double layer structure. However, the derived structure has a sequence, (+)(−)(+)..., which is different from that of the α-form. The presence of water vapour is indispensable in this reaction, and the actual mechanism of transformation thus seems to be complicated.

The author wishes to express his sincere gratitude to Prof. T. Ito for his suggestions and encouragement. He also wishes to express his thanks to Prof. R. Sadanaga and also to Dr M. Tsuboi who gave valuable suggestions.

References

Albrecht, G. & Corey, R. B. (1939). *J. Amer. Chem. Soc.* **61**, 1087.

BERGHUIS, J., HAANAPPEL, IJ. M., POTTERS, M., LOOPSTRA, B. O., MACGILLAVRY, C. H. & VEENENDAAL, A. L. (1955). *Acta Cryst.* **8**, 478.
BERNAL, J. D. (1931). *Z. Kristallogr.* **78**, 363.
COCHRAN, W. (1951). *Acta Cryst.* **4**, 408.
CRUICKSHANK, D. W. J. (1949). *Acta Cryst.* **2**, 65.
CRUICKSHANK, D. W. J. (1956). *Acta Cryst.* **9**, 757.
DARWIN, C. G. (1922). *Phil. Mag.* **43**, 800.
DONOHUE, J. (1950). *J. Amer. Chem. Soc.* **72**, 949.
FISCHER, E. (1905). *Ber. dtsch. chem. Ges.* **38**, 3, p. 2917.
IITAKA, Y. (1953). *Acta Cryst.* **6**, 663.
IITAKA, Y. (1954). *Proc. Japan Acad.* **30**, 109.
IITAKA, Y. (1958). *Acta Cryst.* **11**, 225.
IITAKA, Y. (1959*a*). *Nature, Lond.* **183**, 390.
IITAKA, Y. (1959*b*). *Miner. J.* **2**, No. 5, 283.
IITAKA, Y. (1959*c*). To be published.
KSANDA, C. J. & TUNELL, G. (1938). *Amer. J. Sci.* A, **35**, 173.
LIPSON, H. & COCHRAN, W. (1953). *The Crystalline State*, vol. 3, p. 288. London: Bell.
MARSH, R. E. (1958). *Acta Cryst.* **11**, 654.
PASTERNAK, R. A., KATZ, L. & COREY, R. B. (1954). *Acta Cryst.* **7**, 225.
SHOEMAKER, D. P., DONOHUE, J., SCHOMAKER, V. & COREY, R. B. (1950). *J. Amer. Chem. Soc.* **72**, 2328.
SHOEMAKER, D. P., BARIEAU, R. E., DONOHUE, J. & LU, C.-S. (1953). *Acta Cryst.* **6**, 241.
TSUBOI, M., ONISHI, T., NAKAGAWA, I., SHIMANOUCHI, T. & MIZUSHIMA, S. (1958). *Spectrochim. Acta*, **12**, 253.
YAKEL, H. L., JR. & HUGHES, E. W. (1952). *J. Amer. Chem. Soc.* **74**, 6302.

Acta Cryst. (1960). **13**, 45

The Structure Analysis of a Guinier–Preston Zone by Means of a Fourier Method

BY KENJI DOI*

Mineralogical Institute, Faculty of Science, University of Tokyo, Hongo, Tokyo, Japan

(*Received* 24 *November* 1958 *and in revised form* 28 *March* 1959)

The structure of a G.–P. zone in Al–Cu alloy was analysed using a Fourier transformation of the *amplitude* distribution near the reciprocal lattice point (200). For each atomic plane composing the zone, the content of Cu atoms and the displacement from the net plane of the matrix crystal have been determined. The Cu content was found to vanish after the second plane from the origin, giving the zone a quasi-two-dimensional structure. A displacement of about 0·15 Å toward the zone origin takes place for the first plane, and displacements for the other planes are found to be negligible. The results are compared with those previously obtained by Toman and by Gerold.

Introduction

The analysis of scattering patterns produced by imperfections in crystals has been carried out usually either by (i) the comparison of observed intensities with those calculated on more or less arbitrary structure models by trial and errors, or by (ii) Fourier transformation of the observed *intensity* distribution (see, for example, Guinier, 1956). The second method can be carried out with less detailed assumptions than the first, though the information it furnishes is related only to the atom pairs present in the crystal and not directly to the atomic arrangement.

The present author (Doi, 1957) proposed previously a method of analysing the disordered structures by Fourier transformation of the *amplitudes* of scattered X-rays in a limited region of reciprocal space, e.g. the region surrounding a relpoint, and showed that the information concerning the atomic arrangement in the disordered crystal may be obtained to some extent directly from the intensity distribution of the scattered X-rays, as the phase angles of the amplitudes in the region concerned may be determined by a similar method to that applied by Li & Smoluchowski (1954) for the analysis of small-angle scattering. In the present paper the theory is applied to the structure analysis of the Guinier–Preston zone (which is quoted hereafter as G.–P. zone).

* Present address: Japan Atomic Energy Research Institute, Tokai-mura, Naka-gun, Ibaraki-ken, Japan.

2. Principle of analysis

Let us consider the following function related to a one-dimensional structure of unit translation a,

$$\varphi_H(x)=\int_{-\infty}^{+\infty} A(s)K(s-s_H)\exp 2\pi i x(s-s_H)ds\,, \quad (1)$$

where

$$K(s)=\frac{\sin \pi as}{\pi s} \quad (2)$$

in place of the usual expression for electron densities